Geological Magazine

www.cambridge.org/geo

Past and present biodiversity correlates with spatial environmental gradient

Giulia Bernardini[1,2], Gareth G. Roberts[1] and Mark D. Sutton[1]

[1]Department of Earth Science & Engineering, Imperial College London, London, UK and [2]Grantham Institute for Climate Change and the Environment, Imperial College London, South Kensington Campus, London, UK

Original Article

Cite this article: Bernardini G, Roberts GG, and Sutton MD. Past and present biodiversity correlates with spatial environmental gradient. *Geological Magazine* **163**(e7): 1–13. https://doi.org/10.1017/S0016756825100502

Received: 12 November 2025
Revised: 2 December 2025
Accepted: 16 December 2025

Keywords:
Paleoecology; ecology; environmental gradients; biodiversity patterns; landscape variation

Corresponding author:
Giulia Bernardini;
Email: giulia.bernardini18@imperial.ac.uk

Abstract

Recent palaeobiological studies have emphasized the need for interpretations of the fossil record to consider spatial changes in environmental conditions (e.g. topography, climate). Establishing the role the environment plays in determining the distributions of extinct and existing organisms is complicated by biological evolution. Using available observations to 'see through' the randomness of biological evolution to determine contributions from environmental change is not trivial because of the sparsity of the fossil record, lack of precise information about rates of evolution, and because we obviously cannot physically re-run the evolutionary history that resulted in modern biodiversity or the fossil record. To address these issues, we establish scales and scenarios in which spatial environmental change is manifested in records of the number of species in a given area (richness) generated by eco-evolutionary simulation. Evolutionary processes that are likely to be random on the timescales of environmental change are included. Signals of environmental change that are likely to be hidden by the effects of 'noisy' evolutionary processes and those likely to emerge are identified. The 'experiment of life' is simulated many times, producing statistical insights. Results show that the spatial rate of environmental change is strongly correlated with species richness when the ability of organisms to disperse is high. Interaction between scale, dispersal and environmental structure is shown to determine both statistical and spatial distributions of richness. As a proof-of-concept, we compare predictions to bird species richness. The results emphasize the need to consider the randomness of evolution when interpreting the observations of extinct or present life on Earth.

1. Introduction

Understanding the drivers of biodiversity across spatial scales remains a central challenge in ecology and evolutionary biology (see e.g., Benson *et al.* 2021; Mannion *et al.* 2014). While many empirical studies have established that extant species distributions are influenced by both abiotic (e.g., temperature, elevation and precipitation) and biotic factors, the underlying mechanics of these relationships remain difficult to disentangle (see e.g., Antonelli *et al.* 2018; Mitchell *et al.* 2024). These difficulties arise because biodiversity patterns are the result of a single 'experiment', comprising a complex history of variation in many environmental variables, as well as a particular evolutionary history (e.g., Benson *et al.* 2021; Benton, 2009; Willig *et al.* 2003).

Correlative approaches comparing extant species range maps to environmental data have shown associations between environmental heterogeneity and species richness (e.g., Stein *et al.* 2014; Tuanmu & Jetz, 2015). These studies often highlight the role of spatial gradients and identify relationships that vary with spatial scale and taxonomic group (Belmaker & Jetz, 2011; O'Malley *et al.* 2023). However, such correlations do not clarify whether the environment causally drives richness patterns, or whether both variables are structured by spatial autocorrelation, range size effects or historical contingency (Cabral *et al.* 2017). Understanding how correlations arise, how they change as functions of space and scale, and establishing how, or even if, the environment is significant in determining patterns of species richness across the scales of interest (individuals to continents) are problems to be solved. A general challenge is that areas with similar environmental conditions can contain different numbers of species, demonstrating that local environmental conditions alone do not determine species richness (Koenig, 1999).

There are two fundamental and separate challenges in inferring causality from empirical biodiversity data. The first of these is that many variables contribute to biodiversity patterns. They can be complex and interrelated. They are imperfectly understood, and their histories are at best partially known. Empirical studies have limited control over these variables and hence struggle to isolate their individual effects. The second problem arises from the stochastic nature of evolutionary processes (e.g., genome mutation/drift, organism dispersion; Willig *et al.* 2003). Even if the 'experiment of life' could be run repeatedly from the same starting point and using the same environmental variables, the stochasticity of evolution would likely result in different eco-evolutionary histories and hence different biodiversity patterns. Empirical studies can make

© The Author(s), 2026. Published by Cambridge University Press. This is an Open Access article, distributed under the terms of the Creative Commons Attribution licence (https://creativecommons.org/licenses/by/4.0/), which permits unrestricted re-use, distribution and reproduction, provided the original article is properly cited.

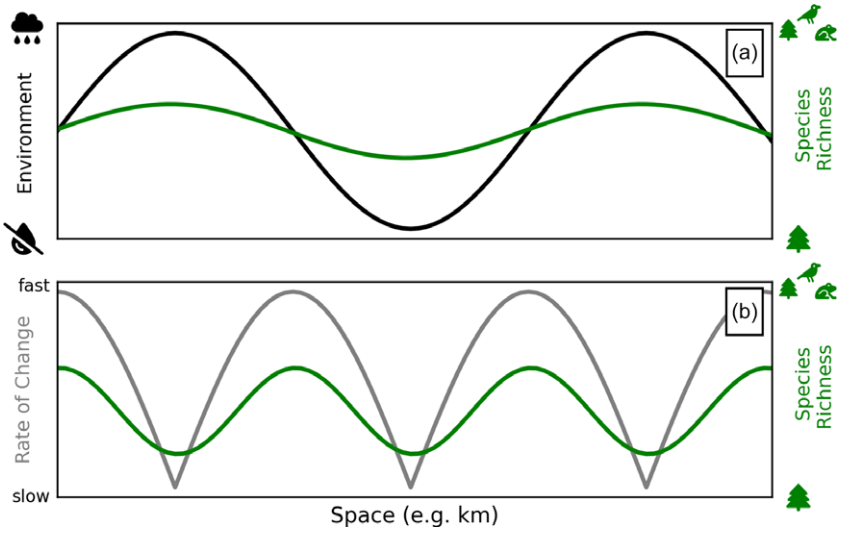


Figure 1. Simplified postulated relationships between environment and species richness tested in this study. (a) Species richness (green) has a simple and direct relationship with environment (black). More formally, species richness is in-phase with the environment. (b) Species richness (green) has simple and direct relationship to environmental rate of change (strictly, the absolute value of the spatial derivative; grey). Strictly, we consider the absolute value of the derivative of the environmental variable (cf. black and grey curves).

use of only one 'run' of the experiment. Thus, they provide limited insight into statistical properties of the system and little information about whether the 'run' that generated the observations was typical or anomalous. This lack of information confounds attempts to infer causal relationships between the environment and biodiversity of extant or extinct organisms, as the effects of a particular contingent history cannot be excluded.

To address both of these problems and for consistency, we explore the use of organism-level simulations to investigate how dispersal ability and environmental gradients interact to shape biodiversity patterns. We build on a body of work that has developed the means to predict biodiversity in space and time from evolutionary 'first principles'. For instance, Gotelli *et al.* (2009) and Rangel *et al.* (2018) provide methodological frameworks using simulations to understand theoretical and observed macroecological patterns, including biodiversity in the South American continent. The potential of mechanistic approaches to predict biodiversity has been emphasized by Connolly *et al.* (2017), Pontarp *et al.* (2019) and Dolson & Ofria (2021). Catella & Abbott (2023) explored how abiotic heterogeneity influences species densities and spatial biodiversity patterns in digital simulations. Bridle *et al.* (2010) showed that dispersal, gradient steepness and carrying capacity can be key determinants of adaptation.

In contrast to modelling approaches that operate at the species level or higher (cf. Gotelli *et al.* 2009; Rangel *et al.* 2018; Ruffley *et al.* 2019; van der Plas *et al.* 2015), organism-level simulation does not require assumptions about patterns and processes at a higher organizational level (Pontarp & Wiens, 2017). Instead, such patterns arise from the behaviour of individuals, as they do in nature (e.g., Dolson & Ofria, 2021). While many previous simulation studies rely on only one or a few replicates, we explore whether well-defined statistical distributions emerge when a very large number of experiments containing stochastic evolutionary processes are conducted. By running many 'experiments of life' as computational simulations, we are able to isolate and control environmental variables and to develop statistical expectations for biodiversity over a large number of different evolutionary histories. This approach permits assessment of the 'strength' of the relationship between richness and environmental gradients and how it is influenced by evolutionary stochasticity.

Specifically, our study tests whether the spatial rate of environmental change emerges as a useful metric to predict biodiversity and under what conditions this relationship holds. To simplify our study, we use a single (abstract) environmental variable, varying spatially in a sinusoidal manner. We quantified the spatial rate of change as the absolute value of the first derivative of this variable; for brevity, we term this metric the *spatial derivative*. The abstract environmental variable might be conceived of as altitude, for example, in which case the spatial derivative would represent the topographic slope. We test whether linkages between the spatial derivative and biodiversity emerge consistently across replicated simulations when dispersal is sufficient to allow organisms to track environmental variation without homogenizing diversity (Figure 1).

We employ the rapid evolutionary simulator (REvoSim; Garwood *et al.* 2019), an individual-level simulation model where phenomena such as speciation and adaptation can emerge from evolutionary first principles. REvoSim is computationally efficient – whilst it operates at the level of individual organisms, it can simulate populations of $10^5 - 10^7$ species in spatially structured environments over geological timescales on a typical desktop computer. Simulated organisms evolve through changes within a fixed-length genome (first-order evolution, *sensu* DeJong & Degens, 2024). This model has been used by others to test ideas about the relationship between environmental instability, disturbance and biodiversity (Furness *et al.* 2021a; Furness & Sutton, 2024). By omitting complex interactions like predation or mutualism, REvoSim provides a controlled environment to test whether such complexities are essential for producing the observed macroecological patterns. It has been used to understand how productivity, niche availability and other factors influence species richness and extinction risk in ecosystems (Furness *et al.* 2021b). It can replicate observed phenomena, e.g. species richness patterns and genetic diversity that mimic observations from the real world whilst honouring the fundamental principles of evolution, making it well suited for our goals (see e.g. Garwood *et al.* 2019).

REvoSim represents each organism with a fixed-length binary genome (64 bits in this study). Each organism is located within a specific 'cell' in a two-dimensional, spatially structured environment. The first 32 bits of the genome are used to assess the fitness of the organism to the environment; all 64 bits are used to assess reproductive fitness and to identify species. Reproduction is determined by the similarity of the genomes of individuals and the values of environmental variables in the cell. The reader is referred

https://doi.org/10.1017/S0016756825100502 Published online by Cambridge University Press

to (Garwood *et al.* 2019) for full details of the REvoSim model and software implementation. For convenience, a summary of the methodology relevant to this study is given as in the Supporting Information.

We note that many metrics and proxies for biodiversity are available (see e.g., DeLong, 1996). For instance, the diversity of genes within a group of organisms (genetic diversity) and the count of unique species occupying a specific area (species richness) are both used to assess the variety of life. Although species richness has been criticized as a metric for assessing biodiversity because it does not account for relative abundance, genetic variation or functional traits (see e.g., Gotelli *et al.* 2009; Hillebrand *et al.* 2018), it remains widely used, partly because it is relatively easy to determine from real-world data and can also be estimated in a palaeontological context (see e.g., Benson *et al.* 2021 and references therein). In this study, we use species richness, which we assess by counting the number of species within a cell. Given that genetic information is available for every individual in a simulation, we also explore the extent to which species richness correlates with genetic diversity.

Comparisons with data from current-day biota reduce uncertainties that would be associated with interpreting the relatively sparsely sampled history of biodiversity preserved by the fossil record (see e.g., Alroy, 2008; Alroy *et al.* 2001). To provide an example of how predictions from REvoSim can be tested against real-world data, we thus analyze extant avian species richness along an equatorial African transect. This region appears to have been broadly geologically and climatically stable, occupying similar latitudes, during the last few million years, increasing compatibility with assumptions in our simulations (e.g., Dagallier *et al.* 2020; Jetz *et al.* 2004; Burke, 1996). We test whether species richness along this transect correlates more strongly with the *spatial derivative*, e.g. the slope of elevation, precipitation or temperature, than with the values of modern environmental variables, acknowledging that these parameter values can change in time (e.g., deMenocal, 2004). This analysis is provided as a demonstration of how findings from a synthetic model can be linked to detailed empirical biodiversity data. We speculate on how it might be useful for interpreting the fossil record.

In summary, we use replicated, mechanistic simulations to clarify when and how the spatial structure of environments can be straightforwardly related to biodiversity. We establish when 'noise' introduced by evolutionary stochasticity conceals the relationship. By isolating the roles of dispersal, environmental variables, and stochastic evolutionary processes, we provide a framework for interpreting large-scale biodiversity patterns beyond classic correlative approaches. Our findings help define the limits of predictability imposed by stochastic evolutionary processes and demonstrate how synthetic models can be used to contextualize the partial information about ancient biodiversity preserved in the fossil record.

2. Methods

2.a. Modelling strategy

In REvoSim, the organisms can reproduce and mutate. Each individual is defined by a 64-bit binary genome, a sequence of zeros and ones (genes). Genomes within populations evolve through stochastic mutation. Genes are also subject to adaptation through selection for fitness in the environment. Organisms reproduce sexually with other organisms in the same cell. Species are automatically identified by REvoSim using the Biological Species Concept, i.e. as reproductively-isolated population groups (Garwood *et al.* 2019). When the genetic difference between two organisms exceeds a configurable threshold, they are not able to breed and are classified as distinct species.

We explore simple models in which the environment, e, is determined by integer values, $0 \leq e \leq 255$, in a uniform grid of $X \times Y$ cells or pixels (px), where $X = Y = 100$. REvoSim maps environmental parameter values to colors in a raster image for visualization purposes. We use an environmental map that varies sinusoidally in the x direction and is constant in the y direction. This setup is analogous to real-world scenarios where organisms must adapt to a single environmental variable that changes along a single spatial dimension. We set the spatial grid to be toroidal, i.e. to 'wrap around' in both x and y directions, to avoid edge-effects (Porensky & Young, 2013). The sinusoidal wavelength chosen ($\lambda = 50$ px) provides this 'wrap around' in the x direction without discontinuities (Figure 2f).

In a series of systematic experiments, we varied the capability of organisms to disperse. REvoSim default settings were otherwise used for all other parameters. At the start of each experiment, a population of genetically identical organisms was inserted into the cell at the centre of the environment, where they started reproduction, mutation and dispersal. The experiments were then iterated for $T = 100,000$ steps, which could represent $O(0.1 - 1$ Myr) of vertebrate evolution. Species richness broadly increased in each experiment until $\sim$50,000 steps, after which it typically stabilized (Figures 2a–e & 3). Replicate experiments ($N = 3000$) were produced for each scenario (i.e. for each dispersal setting). This Monte Carlo experimentation allows statistical understanding of expected species richness from models incorporating evolutionary stochasticity, which can experience very different trajectories across replicates (Figure 3).

2.b. Evolutionary stochasticity

REvoSim experiments included four sources of stochasticity. Two represent per-replicate determination of initial conditions, specifically generation of a 'fitness landscape' (McCandlish, 2011; McGhee, 2006), and selection of a viable genome for the initial population (see Garwood *et al.* 2019). Stochasticity *during* each replicate occurred in mutation (see Garwood *et al.* 2019) and in dispersal; the latter is discussed here in more detail.

REvoSim organisms do not move, but offspring of reproductive events 'disperse', i.e. attempt to establish themselves either in the same pixel as their parents, or in a nearby pixel. The dispersal distance is defined as

$$D = \left|\frac{C}{d}\right|, \tag{1}$$

where the dispersal parameter, d, is set at the beginning of each experiment and is constant for all organisms. The parameter $C = \sqrt{65536/(b+1)} - 16$ controls the stochasticity of dispersal via the value of b, which is chosen randomly from a uniform distribution $0 \leq b \leq 255$ (thus $0 \leq C \leq 240$). In practice, displacement is determined by defining translation along the x and y axes

$$D_x = \frac{C}{d}\sin(\alpha),\ D_y = \frac{C}{d}\cos(\alpha) \text{ thus } D = \sqrt{D_x^2 + D_y^2}, \tag{2}$$

with the azimuth of displacement, $0° < \alpha \leq 360°$, chosen randomly from a uniform distribution (Garwood *et al.* 2019).

https://doi.org/10.1017/S0016756825100502 Published online by Cambridge University Press

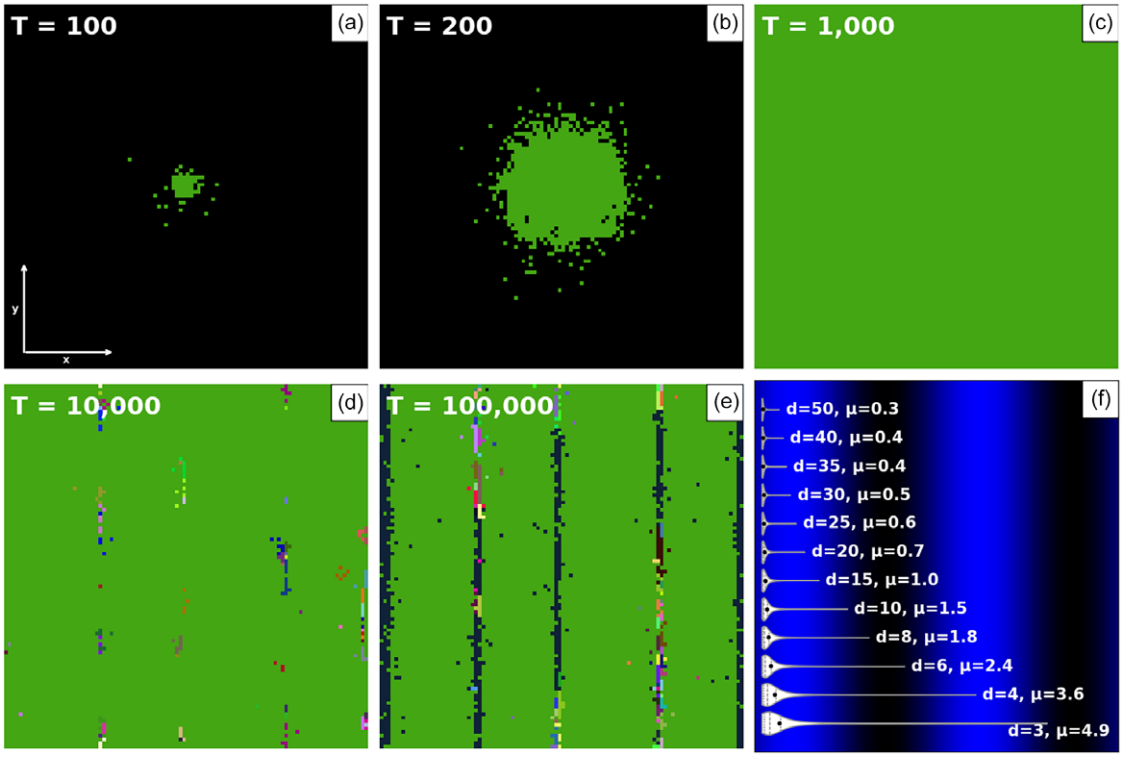


Figure 2. An example of species dispersion in a single simulation and dispersion parameters included in this study. (a-e) Biodiversity in a single simulation after 100, 200, 1000, 10,000 and 100,000 steps. This simulation has spatial dimensions of 100×100 pixels (white vectors in panel a; see body text for extended description). Colors correspond to the most abundant species in a pixel at any given time; colors for species are chosen arbitrarily. Black indicates no organisms present. (a-b) The first organism (green), inserted into the centre of the domain, reproduces and disperses to other pixels. (c) Colonization of the whole domain. (d-e) Different colors show that speciation has occurred and new species are now most abundant in certain pixels. (f) Map showing the simple sinusoidal environment and dispersion parameters, d, used to control dispersion of offspring in this study. White violin plots show probabilities of dispersion for each dispersion parameter at the scale of the environment; black dots = mean dispersion, μ. $d = 15$ for simulation shown in panels (a–e). See body text for details.

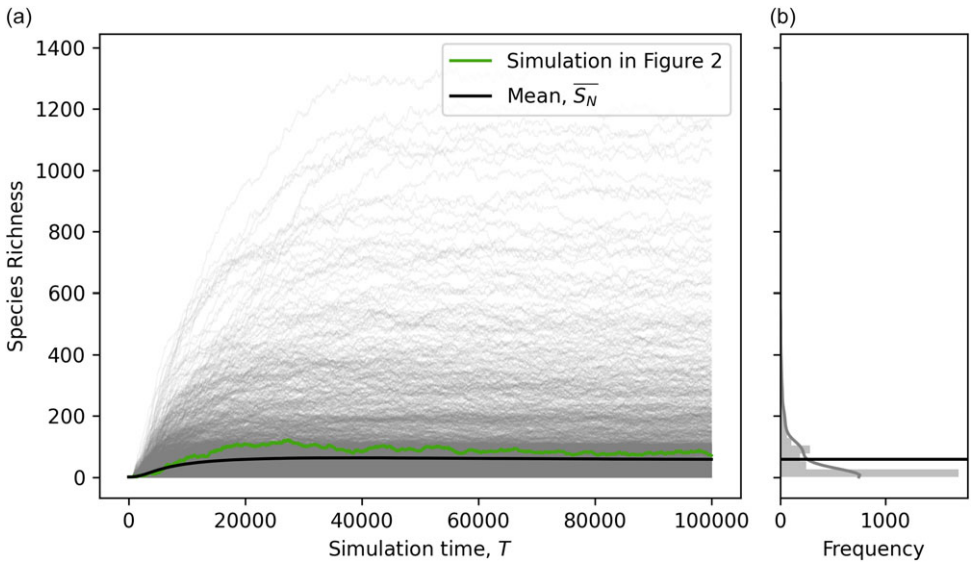


Figure 3. Variability of species richness in time from Monte Carlo experimentation. (a) Grey curves = species richness as a function of time in $N = 3000$ simulations. Environmental variable ($\lambda = 50$ px) and dispersion parameter ($d = 15$; see Figure 1f) were held constant. Gene mutation, reproduction and dispersion are stochastic (see body text for extended description). Green line = trajectory of simulation depicted in Figure 1a–e. Black line = mean species richness, $\bar{S}$, from the 3000 simulations. (b) Grey histogram and black line = distribution of species richness and $\bar{S}$ at $T = 100,000$, respectively.

The dispersal of an organism is inversely proportional to d, with minimum and maximum values of zero px and $D_{max} = 240/d$ px, respectively. The distribution of dispersal distances is weighted towards low values. The values of d used in this study, along with associated dispersal distributions and mean dispersal, μ (px), are given in Figure 2f. Figure 2a–e shows an example of species spreading across the model domain (via reproduction and dispersal), during $100,000$ time steps; in this example, the probability that offspring will disperse to within $D = 2$ px of their source pixel (containing their parents) is 88%.

As an example, Figure 3a shows species richness trajectories for all replicates for one parametrization of dispersal ($d = 15$). Mean

https://doi.org/10.1017/S0016756825100502 Published online by Cambridge University Press

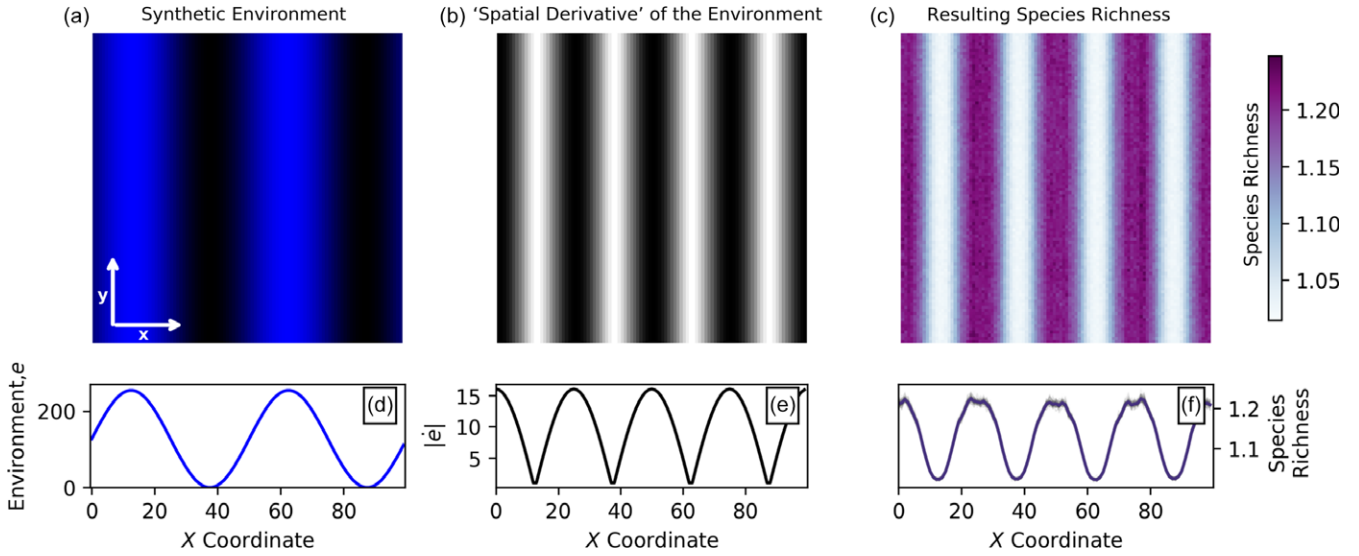


Figure 4. Distribution of species richness at steady-state from Monte Carlo experimentation. (a) Environment; blue/black = high/low values; $\lambda = 50$ px. (b) Absolute values of the derivative of the environment; white/black = low/high. (c) Mean species richness for each pixel at $T = 100,000$ steps from the 3,000 simulations ($d = 15$; see Figure 2f). (d) and (e) transects across the centre of the environment (panel a; at $y = 50$) and the absolute values of its derivative (b), respectively. (f) Transects across mean species richness shown in panel (c); grey curves = transects at $y = 1, , 100$; purple curve = mean species richness for all 100 transects.

species richness for all replicates (black curve) and the experiment shown in Figure 2a–e (green curve) is indicated. Figure 3b shows the distribution of species richness for all replicates with $d = 15$.

2.c. Metrics of species richness and genetic diversity

Two types of logs were generated for each individual experiment. The first type records species richness every 50 time steps (referred to as 'species counts' by REvoSim). These were configured as 'v2.0.0 CSV' logs in REvoSim settings, and were used to extract species richness across the grid. The second type records the genomes, species identifications and spatial locations for all individuals present at the final step ($T = 100,000$). These were used to calculate the mean species richness at each pixel and to calculate genetic diversity across the grid.

Species richness for each pixel in each replicate was calculated by counting the unique number of species present in that pixel. These results are used to calculate mean species richness at each x position on the grid (i.e. averaging over all y pixels for each x position), for each value of d (see Figure 4f). Species richness for the whole domain was also calculated for each replicate by counting the unique number of species present in the whole 100×100 pixel grid. These values were then compared with the genetic diversity of the corresponding replicate.

We used the following terminology to describe species richness. $S(x, y)$ refers to the species richness of cell (x, y) for a particular value of d, in a particular replicate n. See Figure S1 shows a schematic of the model setup and associated statistics. All of the following statistics were calculated using only the N replicates that had extant species at $T = 100,000$. In practice, more than 92% of all simulations are included in these results.

$\bar{S}(x, y)$ is the mean species richness of cell (x, y) for a particular value of d. S_n is the number of unique species across the entire grid for an individual replicate, n. $\overline{S_N}$ is the mean number of species across the entire grid for a particular value of d, over all replicates, $\overline{S_N} = \frac{1}{N}\sum_{n=1}^{N} S_n$. $\overline{S_x}$ is the mean species richness as a function of x, for a particular value of d incorporating all replicates. This value is calculated as the mean of $\bar{S}(x, y)$ for a given x. For example, at $x = 50$, $\overline{S_{x=50}} = \frac{1}{NY}\sum_{y=1}^{Y}\sum_{n=1}^{N} S_n(x = 50, y)$. $\overline{S_{xmax}}$ is the maximum value of $\overline{S_x}$ for a specific value of y and d. In addition, we calculated the normalized value of mean species richness as a function of x, calculated using min–max feature scaling, $(\overline{S_x} - \overline{S_{xmin}})/\ (\overline{S_{xmax}} - \overline{S_{xmin}})$ and annotated as $\overline{S_x}/\overline{S_{xmax}}$ for simplicity. This normalized value is used to compare $\overline{S_x}$ across the different values of d.

Mean genetic diversity in a single replicate, $\overline{\pi}_n$, was calculated by comparing genomes from M pairs of individuals,

$$\overline{\pi}_n = \frac{1}{M}\sum_{m=1}^{M}\sum_{i=1}^{64} |I_1^{i,m} - I_2^{i,m}|, \tag{3}$$

where I_1 and I_2 are the individuals whose genomes were compared, and $i = 1, 2, , 64$ is the index of genes for each genome for each individual. Since genes are binary digits (either 0 or 1), $\overline{\pi}_n = 0$ when all individuals are genetically identical. For theoretical scenarios in which all individuals have completely different genomes $\overline{\pi}_n = 64$. It is possible to calculate the true mean genetic diversity for each replicate. However, as the number of individuals present during each replicate (I) can exceed 100,000, the total number of unique pairs $(I(I-1)/2)$ can exceed 10 billion, rendering exhaustive comparison computationally impractical. Instead, we estimated $\overline{\pi}_n$ from a sample of the total number of pairings, by comparing $M = I/2$ randomly chosen unique pairs. Thus, we typically compared $> 90,000$ pairs of individuals for each replicate. Figure 5 plots mean genetic diversity for each replicate, $\overline{\pi}_n$ compared with its respective species richness, S_n.

2.d. Real-world data

An equatorial transect of Africa is used to demonstrate how results from simulation can be used to contextualize real-world

https://doi.org/10.1017/S0016756825100502 Published online by Cambridge University Press

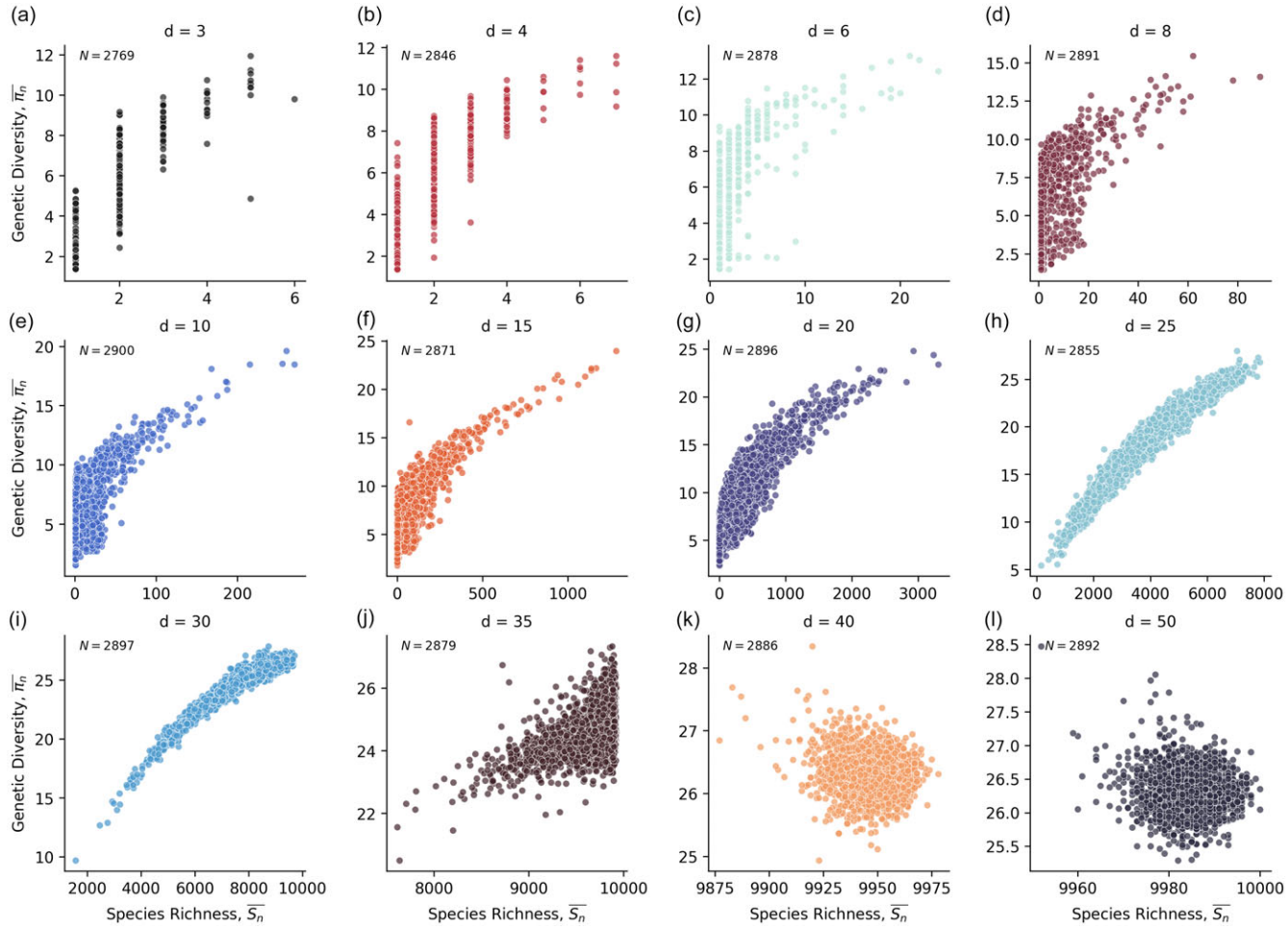


Figure 5. Genetic diversity versus species richness at equilibrium. (a) Species richness and genetic diversity compared at $T = 100,000$ for N replicates with dispersion parameter $d = 3$ (see Figure 6a). (b–l) Results for different values of dispersion parameter (annotated).

observations (see Figure S5). Mean annual precipitation, temperature and temperature range from 1981–2010, were extracted from the *Climatologies at high resolution for the Earth's land surface areas* (CHELSA) dataset (Karger *et al.* 2017) at a resolution of 30 arcseconds ($\approx$ 1 km at the equator). We note that CHELSA data have been used in previous studies modelling species distributions (e.g., Doninck *et al.* 2020; Karger *et al.* 2017; Morales-Barbero & Vega-Álvarez, 2019). Elevation data were extracted from ETOPO1 (Amante & Eakins, 2009), with a resolution of 1 arcminute ($\approx$ 2 km at the equator). The derivatives of each variable were calculated using the central differences.

For species richness, birds were selected as an exemplar group for their well-documented distribution on the continent (Claramunt & Cracraft, 2015; Fuchs *et al.* 2006; and Oliveros *et al.* 2019) and the availability of data. Avian species richness was extracted from Jenkins *et al.* (2013) expert range map, which has a resolution of 10 $\times$ 10 km.

All transects were sampled from each dataset at 10 km intervals.

Species richness estimates from range maps may be unreliable at fine scales (Cohen & Jetz, 2024; Graham & Hijmans, 2006; Hurlbert & Jetz, 2007). Hurlbert & Jetz, (2007) demonstrate that atlas data and range maps of bird species in Africa correlate well at resolutions $>2^\circ$ ($\approx$ 200 km), which suggests that focusing our analysis on larger scales might be prudent. We therefore removed wavelengths (scales) $\lesssim$200 km using a Gaussian filter before comparing the spatial series. For comparison, we also generate results for wavelengths $\gtrsim$ 1000 km. Pearson's product-moment correlation coefficients and p-values were calculated between avian species richness and (a) environmental variables, and (b) the absolute values of the *spatial derivatives* of the environmental variables.

3. Results

3.a. Mean species richness varies with dispersal ability

Figure 5 shows genetic diversity compared to species richness in simulations at 'equilibrium' (at $T = 100,000$). Diversity and richness covary positively, $Cov(\overline{S_n}, \overline{\pi_n}) > 0$, in simulations that incorporate relatively high dispersal abilities, i.e. $d < 40$: $D_{max} \geq 6$ px, $\mu \geq 0.4$ px. When dispersal ability is relatively low ($d \geq 40$, Figure 5k–l), covariance is close to zero, $Cov(\overline{S_n}, \overline{\pi_n}) \approx 0$. However, this arises because the variance in both metrics is very low, resulting in the covariance being 'swamped' by stochastic noise. These results indicate that, in this system, species richness is a good proxy for genetic diversity. Species richness is the simpler quantity to measure or estimate in empirical data (for both extant and extinct biota; see, e.g., Benson *et al.* 2021; Jetz *et al.* 2012); consequently, we use only species richness in our analyses.

Species richness for the entire domain varied between 1 (only one species present) and 10,000 (all pixels occupied by a different

https://doi.org/10.1017/S0016756825100502 Published online by Cambridge University Press

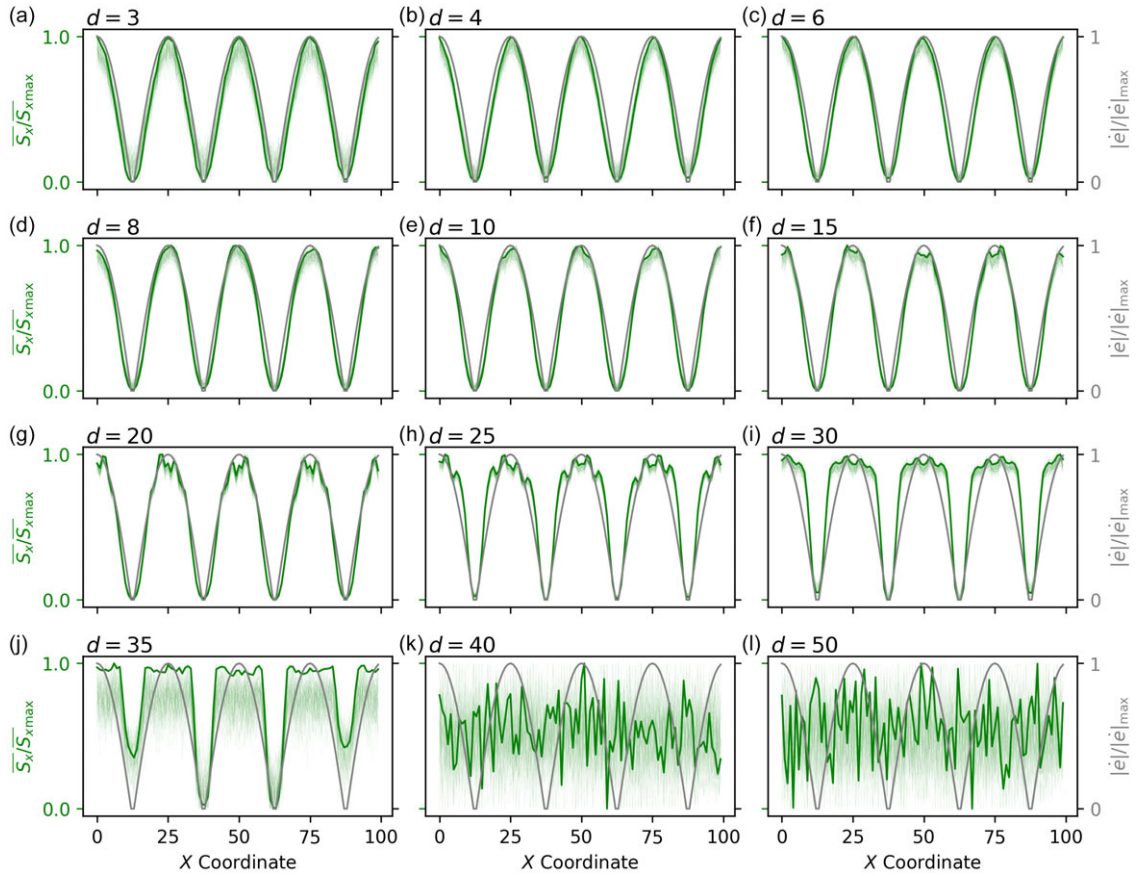


Figure 6. Relationships between environment and species richness as a function of dispersion. (a–l) All simulations used the same environment (see Figure 4; $\lambda = 50$ px). Dispersion ability was varied by systematically changing the value of dispersion parameter, d, see panel annotations and Figure 2f (note low d indicates higher dispersion). Grey curves = absolute value of the derivative of the environmental variable, $|\underline{e}|$, normalized using min-max feature scaling, $(|\underline{e}| - |\underline{e}|_{min})/(|\underline{e}|_{max} - |\underline{e}|_{min})$, as a function of x coordinate (see Figure 4e). Dark green curves = transects of mean species richness, $\overline{S_x}$, (along the x coordinate; see Figure 4f) for 3,000 simulations with given value of d, normalized by using min-max feature scaling $(\overline{S_x} - \overline{S_x}_{min})/(\overline{S_x}_{max} - \overline{S_x}_{min})$. Light green curves = mean species richness transects at $y = 1, \ldots, 100$, calculated from all $\approx 3,000$ experiments, each line normalized using min-max feature scaling.

species) over the full range of experiments. The highest mean species richness, $\overline{S_N}$, at the final step of the model occurred at $d = 50$ ($D_{max} = 4.8$ px, $\mu = 0.3$ px; see Figure S3). Figures 3b and S4 show that frequency distributions of species richness tend to be skewed towards low values for high dispersal ($d \leq 20$, $D_{max} \geq 12$ px, $\mu \geq 0.7$ px), and to be Gaussian or slightly skewed towards higher values for low dispersal ($d \geq 25$, $D_{max} \leq 10$ px, $\mu \leq 0.6$ px).

3.b. Relationship between diversity and environment in simulations

Figure 4 illustrates the spatial distribution of the environmental parameter, e, the absolute value of its derivative $|\dot{e}| = |de/dx|$ (for brevity referred to as the *spatial derivative*), and mean species richness, $\overline{S_x}$, for a representative value of $d = 15$. Visual inspection of these results shows that species richness is highly correlated with the absolute derivative of the environmental parameter, $|\dot{e}|$, rather than with e itself. Normalized results for other values of d are shown in Figure 6. For clarity, $|\dot{e}|$ was normalized by its maximum value such that $0 \leq |\dot{e}|/|\dot{e}|_{max} \leq 1$. The highest value of value of $\overline{S}(x, y)$ was 2.78, recorded for $d = 35$ ($D_{max} = 8$ px, $\mu = 0.5$ px).

Pearson's correlation coefficients, r, between $\overline{S_x}$ and $|\dot{e}|$ are shown for each value of d tested in Figure 7. High correlations ($r > 0.8$) were observed for $d < 35$ ($D_{max} > 7$ px, $\mu > 0.4$ px; cf. Figure 6).

3.c. Relationship between diversity and environment in a real-world transect

Figure 8 shows avian species richness, mean annual precipitation (Pn), elevation (E), temperature (T), temperature range (ΔT) and their absolute derivatives along the African equatorial transect. The respective Pearson's correlation coefficients, r, are annotated for each panel and significance ($p < 0.05$) is indicated by asterisks. Species richness is positively ($0.61 \leq r \leq 0.82$) and significantly correlated with the absolute derivatives of all four environmental variables for wavelengths $\gtrsim 200$ km (Figure 8e–h). We note that correlations between species richness and the absolute derivatives of environmental variables are even higher ($0.75 \leq r \leq 0.92$) at wavelengths $\gtrsim 1000$ km (see Figure S6). In contrast, the only environmental variable examined with significant correlation with species richness is elevation ($r = 0.86$; otherwise $r < 0.1$; Figure 8a–d).

4. Discussion

4.a. Spatial rate of change, species richness and the role of dispersal

Species richness in the simulated ecosystems, and in our exemplar real-world dataset, correlates positively with the spatial derivative, $|\dot{e}|$. In other words, these results reinforce the idea that the intensity

https://doi.org/10.1017/S0016756825100502 Published online by Cambridge University Press

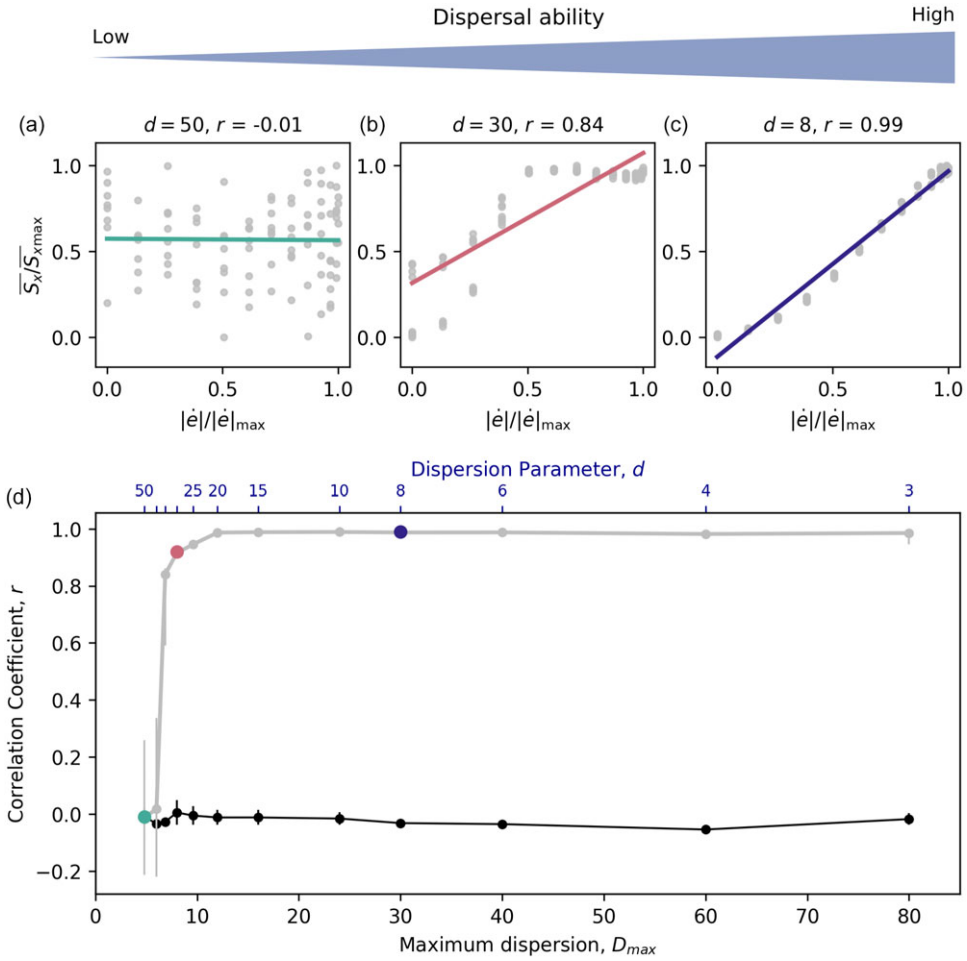


Figure 7. Correlation between mean species richness, derivative of the environment, and environment as a function of dispersion. (a-c) Correlation between normalized mean species richness, $\overline{S_x}/\overline{S_{xmax}}$, and normalized environmental derivative, $|\underline{e}|/|\underline{e}|_{max}$, for $d = 50, 30, 8$. See respective dark green and grey curves in Figure 6. Coloured lines = linear regression, with the correlation coefficient, r, annotated above each plot. (d) Summary of correlation, r, between normalized mean species richness and environmental derivative (grey dots) and environment (black dots) for annotated maximum dispersion, D_{max}, and dispersion parameter, d, values. Error bars = range of coefficients calculated for all, $y = 1, \ldots, 100$, transects in each systematic test of d shown in Figure 6. Coloured dots correspond to panels (a-c).

of spatial variation of an environment appears to be a useful predictor of the number of species within a given area, even when evolutionary processes are permitted to modify biodiversity (cf. Benson *et al.* 2021; Stein *et al.* 2014; Tuanmu & Jetz, 2015). There are two important caveats: first, the dispersal distances of the organisms involved must be sufficiently high. Secondly, a single 'experiment of life' (model realization) may not provide sufficient information to identify this relationship, even if it should be expected (in the statistical sense). It emerges by generating statistical insights, i.e. by running many experiments.

Consider Figure 9, in which the regions (both with spatial range Δx) labelled *i* and *ii* represents areas with low and high environmental variability (Δe), respectively. In other words, the environmental conditions in cells are more similar to their near neighbours in region *i* than in region *ii*. As a consequence, offspring of parents living in cells in region *i* are more likely to be adapted to nearby cells, and thus be able to successfully settle in them. Consequently, gene flow, which requires successful settling in non-parental cells, is greater in region *i* than in *ii*. Gene flow between cells tends to homogenize the genomes of populations; adaptation to their local environments tends to differentiate them, eventually into different species (Coyne *et al.* 2004). The balance between these 'pressures' (or migration-selection balance) appears to determine the prevalence of speciation, which will be favoured in scenarios where gene-flow is inhibited or adaptive pressures (e.g. arising from environmental variation) are high. As the environmental difference between nearby cells in region *ii* (i.e. high $|\dot{e}|$) is greater than that in region *i* (i.e. low $|\dot{e}|$), adaptive differentiation pressures between cells are likely to be greater in region *ii*. Moreover, for the reasons given above, gene flow will be less. Speciation is thus more strongly favoured in region *ii* than in region *i*, and consequently, species richness tends to be higher in region *ii*. Figure 8 demonstrates that a similar relationship appears to exist in the real world, where a steeper environmental gradient, indicative of higher environmental heterogeneity, is associated with greater species richness. This finding aligns with prior studies linking environmental variability to biodiversity patterns of extant species (e.g., Hughes & Eastwood, 2006; Stein *et al.* 2014; Tuanmu & Jetz, 2015). These previous studies analyzed the relationship over patches or areas rather than across a continuous continental transect. While the definition of environmental variability differs across studies, as noted by Stein & Kreft, (2015), to keep the analysis aligned with the scope of this paper, we adopted a straightforward approach, defining it as the mathematical absolute derivative of the environmental variable.

We also find, in simulation experiments, that the coefficient of correlation between $|\dot{e}|$ and mean species richness ($\overline{S_x}$) is related to the dispersal ability of organisms (Figure 7). This phenomenon can also be interpreted in terms of gene flow between cells, which is expected to positively correlate with their ability to disperse (Garant *et al.* 2007). Where dispersal ability is low, gene flow between adjacent cells becomes low because the probability of an offspring attempting to settle in a different cell from its parents is low, e.g. $P(D < 1px) = 94\%$ when $d = 50$ (see Table 1).

https://doi.org/10.1017/S0016756825100502 Published online by Cambridge University Press

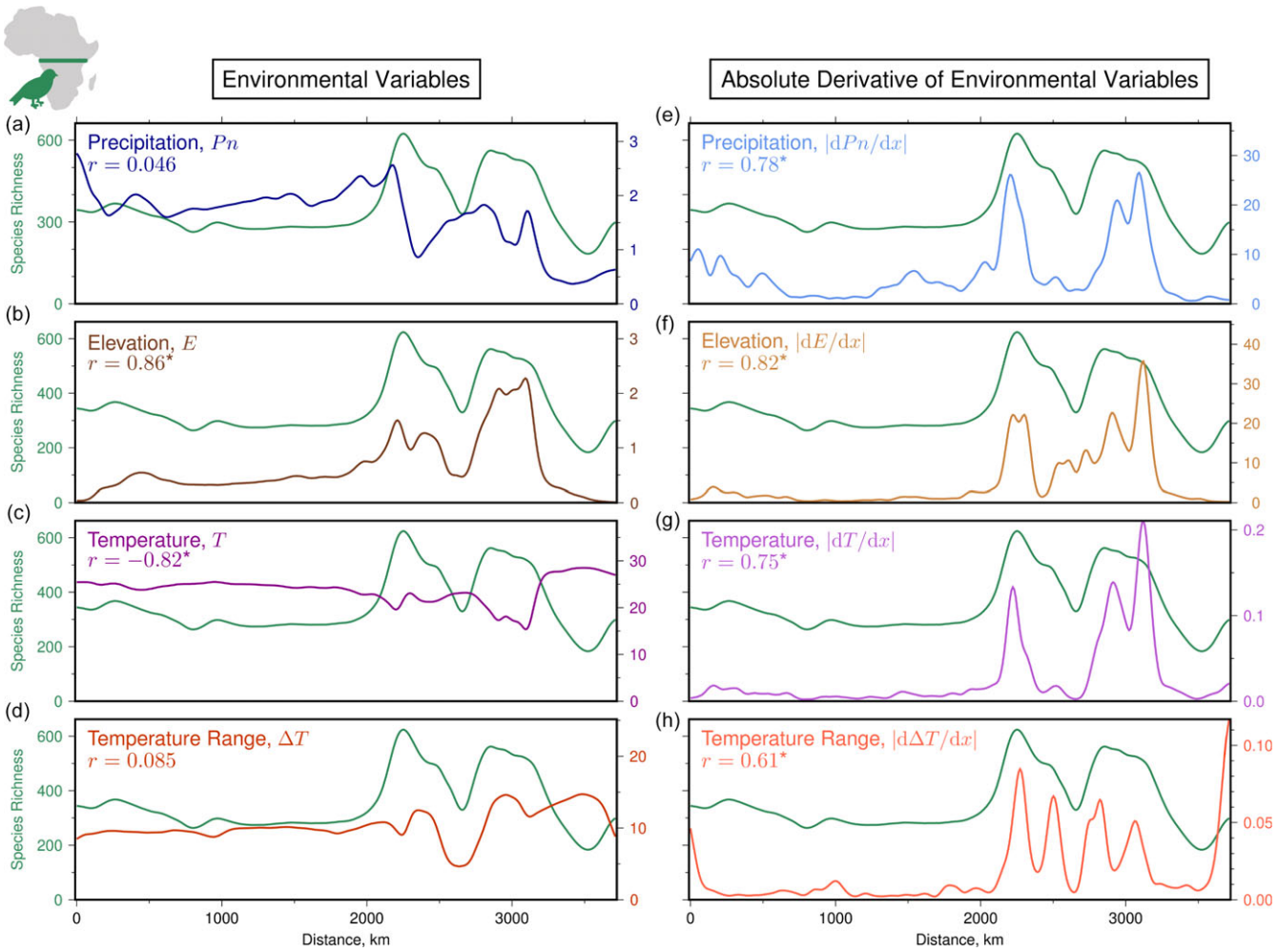
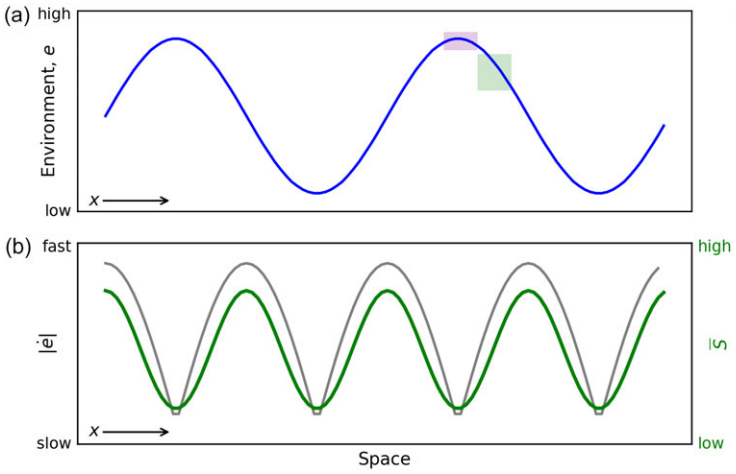


Figure 8. Correlations between Equatorial avian species richness in Africa and precipitation, elevation, temperature, its range and their absolute derivatives. Green curves = avian species richness extracted from Jenkins *et al.* (2013) 10 × 10 km grid, Gaussian filtered to remove wavelengths ≲ 200 km. (a-d) Mean annual precipitation (*Pn*, m), elevation (*E*, km), temperature (*T*, °C) and temperature range (Δ*T*, °C), respectively, from 1981 to 2010 (Amante & Eakins, 2009; Karger *et al.* 2017). All transects were Gaussian filtered to remove wavelengths ≲ 200 km. (e-h) Absolute values of the derivatives of mean annual precipitation (mm/km), topography (m/km), temperature (°C/km) and temperature range (°C/km). Pearson's correlation coefficient (*r*) for species richness and each environmental variable or its absolute derivative are annotated in their respective panels (a-h); asterisks indicate significant p-values ($p < 0.05$). See Figures S5 and S6 for full resolution series and filtering to remove wavelengths ≲ 1000 km.



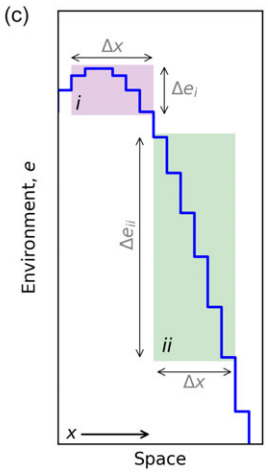


Figure 9. Relationship between environment, its derivative and species richness. (a) Environment, *e*, along the *x*-direction (space; e.g. elevation), see Figure 1. Purple and green boxes refer to the position of i and ii of panel c. (b) Grey line = absolute derivative of the environment, $|\dot{e}| = |de/dx|$, which indicates the spatial rate of change of the environment. Green Line = expected species richness. (c) Model parameterization. Detail from panel a, which shows the discrete values of the simulated environment. Note that Δ*x* is the same for i and ii and that differences in environment Δ*e*, are larger for ii (i.e. $\Delta e_{ii} = 61$) than i (i.e. $\Delta e_i = 12$).

https://doi.org/10.1017/S0016756825100502 Published online by Cambridge University Press

Table 1. Relationships between dispersion and environmental variability.

d	D_{max}	$P(D<1$ px)	r	G
3	80	29%	0.99	5/8
4	60	36%	0.98	5/6
6	40	47%	0.99	5/4
8	30	55%	0.99	5/3
10	24	62%	0.99	25/12
15	16	73%	0.99	25/8
20	12	80%	0.99	25/6
25	48/5	85%	0.95	125/24
30	8	88%	0.92	25/4
35	48/7	90%	0.84	175/24
40	6	92%	0.02	25/3
50	24/5	94%	−0.01	125/12

d = dispersion parameter. $D_{max} = 240/d$ = maximum dispersion (px). r = Pearson's correlation coefficient. G = dimensionless dispersion-environment number.
Note: $\lambda = 50$ (px).

As discussed in the previous paragraph, the likelihood of speciation between any pair of cells is controlled by the relative strengths of gene flow and different adaptive pressures between cells. When gene flow is low (but greater than zero; e.g. $d = 35$; Figure S2j), speciation between cells will become the favoured outcome in cell-pairs even for those with low adaptive differentials (i.e. in regions with low $|\dot{e}|$). When dispersal ability is low, therefore, the importance of the magnitude of adaptive differentials between cells becomes less – most differentials will be sufficiently large to ensure speciation. The correlation between $|\dot{e}|$ and $\overline{S_x}$ is hence weaker when dispersal ability is low, as variation in $|\dot{e}|$ is more weakly tied to the prevalence of speciation.

A feature of our simulation results is that correlation coefficients between $|\dot{e}|$ and $\overline{S_x}$ are consistently very high ($r \geq 0.99$) where d is below a particular value ($d \lesssim 25$; i.e. high dispersal ability). As our experiments use arbitrary units, threshold values of d cannot be directly related to corresponding values in real-world datasets. To facilitate comparisons to the real world, we define a dimensionless parameter, G, that incorporates the ratio of spatial and dispersal scales

$$G = \frac{\lambda}{D_{max}}. \tag{4}$$

D_{max} is preferred here over mean displacement as it is, perhaps, more easily measurable or estimatable for real-world species (extant or extinct). It also captures the spatial range at which gene flow is possible in each time step. Values of G for different dispersal parameters are shown in Table 1. When $G \lesssim 5$, $|\dot{e}|$ is strongly positively correlated with $\overline{S_x}$.

The African transect demonstrates that positive and significant correlations exist between species richness and derivatives of environmental variables at wavelengths $\lambda \gtrsim 200$ km. Inserting this value into Equation (4), $G = 5$ gives $D_{max} = 40$ km. As the maximum dispersal for avian species is likely to be higher than 40 km (Bowman, 2003; Chu & Claramunt, 2023; Sutherland *et al.* 2000), G is likely to be $\lesssim 5$, and thus the recovered correlations fit the predictions of our model.

We note that when $d \geq 40$ in the simulations (i.e. dispersal ability is relatively low) correlation coefficients between $|\dot{e}|$ and $\overline{S_x}$ are close to zero (Table 1; Figure 7). We interpret this result as an artefact of the integer parameterization of e in our study. As discussed above, in any pair of adjacent cells with differing e, speciation will be favoured if differential adaptive pressure arising from the difference in e outweighs the homogenization provided by gene flow. When dispersal ability is low, gene-flow is low, and hence the difference in e between cells required to favour speciation is also lowered. If dispersal ability is lowered sufficiently, the difference in e between cells required to favour speciation may fall to being < 1. Because e is an integer (in the model), the lowest possible difference in e between adjacent cells in the x-direction is 1, except where it is precisely zero; in our environment maps, adjacent cells in the x-direction with differences of e of 0 occur only at minima and maxima. For this reason, in our experiments, there must exist a threshold level of dispersal ability below which all cell-pairs in the x-direction will favour speciation (except the very few where the difference in e is zero), and hence below which the correlation between $|\dot{e}|$ and $\overline{S_x}$ will be very close to zero. We infer that this threshold is between $d = 35$ and $d = 40$ px^{-1}. In the real world, dispersal ability is of course different for different species, and e is not constrained to be an integer. While we infer that the near zero correlations at high d are artefactual due to the integer parametrization, we contend that the less precipitous decreases in correlation where $d \geq 25$ ($G \geq 5$) are not artefacts, as our explanation for their origin does not depend on integer discretization. We expect that high correlations may be observed in real-world datasets between $|\dot{e}|$ and $\overline{S_x}$ where $G \lesssim 5$, and that correlations could be expected to be lower when $G \gtrsim 5$.

4.b. Simplifications and future work

The simulations in this study assume that dispersal capacity is identically distributed for all organisms in each experiment (i.e. d is a constant). This assumption has the obvious benefit of simplifying the assessment of contributions from different driving processes. While we make no claim that this assumption is precisely true in any real-world system, we note that dispersal capacity is frequently observed to be similar within broad clades of extant organisms (Ceresa *et al.* 2016; Matthysen, 2012; Zera & Brisson, 2012). Assuming a constant dispersal distribution may thus be a viable strategy for understanding speciation within many taxa. Similarly, we note that the frequency distribution of dispersal used in our simulations is similar to that of real-world extant organisms in that offspring tend to settle closer to parents, with decreasing frequency at increasing ranges (Matthysen, 2012; Nathan *et al.* 2008; Nathan & Muller-Landau, 2000). The African avian transect examined in this study serves as a single example, focusing on one taxon in a region chosen for its relatively stable environmental conditions over recent geological timescales. This stability facilitates comparisons with models that seek to isolate contributions to species richness from spatial environmental change, as we do here. Further and broader analyses of different taxa and transects are beyond the scope of this preliminary study, but are likely to prove fruitful for interpreting the spatial distributions of extant and extinct organisms. An obvious next step is to consider how we might relate the fossil record directly to results from such simulations, taking into account preservation potential and biases (*sensu* Alroy *et al.* 2001).

First, we suggest that combining experiments of the type presented in this paper with knowledge of dispersal and environmental

https://doi.org/10.1017/S0016756825100502 Published online by Cambridge University Press

variability in the real world could be a way to establish likely distributions of contemporary and ancient biodiversity. Doing so could provide opportunities to develop predictive capabilities to determine species richness across scales. Conversely, interpreting palaeontological records with this framework in mind may support the understanding of environmental change in space and time and quantification of associated uncertainties. A better understanding of linkages could aid in environmental reconstruction from biodiversity patterns. Secondly, a more nuanced understanding of the relationship between spatial structure and biodiversity might be obtained by allowing dispersal ability to vary under genetic control in the eco-evolutionary experiments. Thirdly, an obvious extension is to examine the impacts of more complicated spatio-temporal environmental change on species richness. Future work could incorporate multiple taxa across diverse regions on Earth and make use of insights from dynamic modelling and the geological record to incorporate temporal variability, for instance. Finally, incorporating taxa that occupy similar ranges but are evolutionarily distant, and have different modes of dispersal, could establish an understanding of how such traits impact relationships between environments and biodiversity.

5. Conclusions

By repeatedly running the 'experiment of life' with models of evolution that incorporate random dispersal, mutation and a static environment, statistical insights into the relationships between species richness and spatial environmental variability are established. The results show that, in such systems, species richness should be expected to correlate with the spatial rate of change (strictly, the spatial derivative) of the environment. The strength of the correlation is principally dependent on two factors: the dispersal ability of the organisms and the spatial scale of environmental variables. The role of these factors can be understood through established ecological and evolutionary mechanisms. We demonstrate how that relationship can help to contextualize a transect of real-world present-day species data, demonstrating that, under certain circumstances, our findings are applicable outside the realm of simulation. The results suggest that such an approach may be useful for contextualizing the fossil record or for using the fossil record to reconstruct past environments. When the scale of environmental change is sufficiently small compared to the distance organisms can disperse, the scale of environmental change can reliably predict the distribution of species richness across an environment. We emphasize that these relationships might not be apparent in single experiments or observations generated from sparse fossil assemblages, for instance, because of the randomness of biological evolution. Instead, it is the statistical properties that arise from running many experiments that provided the information needed to identify the relationships and generate the predictions presented in this study. We suggest that it could be fruitful to establish statistical relationships between rates of environmental change and species richness across scales in the modern and ancient real world.

Supplementary material. The supplementary material for this article can be found at https://doi.org/10.1017/S0016756825100502.

Acknowledgements. Thanks to Francois van Schalkwyk for the HPC support and Dr Sameer Bansal for the coding review.

Financial support. G.B. is supported by the Natural Environment Research Council (NE/S007415/1).

Competing interests. The authors declare none.

AI contributions to research content. The authors declare that large language models were used, when necessary, to assist in debugging the Python code.

References

Alroy J (2008) Dynamics of origination and extinction in the marine fossil record. *Proceedings of the National Academy of Sciences* **105**(supplement_1), 11536–42. https://doi.org/10.1073/pnas.0802597105

Alroy J, Marshall CR, Bambach RK, Bezusko K, Foote M, Fürsich FT, Hansen TA, Holland SMIvany LC, Jablonski D, Jacobs DK, Jones DC, Kosnik MA, Lidgard S, Low S, Miller AI, Novack-Gottshall PM, Olszewski T D, Patzkowsky ME, ... Webber A (2001) Effects of sampling standardization on estimates of Phanerozoic marine diversification. *Proceedings of the National Academy of Sciences* **98**(11), 6261–66. https://doi.org/10.1073/pnas.111144698

Amante C and Eakins BW (2009) ETOPO1 arc-minute global relief model: Procedures, data sources and analysis. https://repository.library.noaa.gov/view/noaa/1163

Antonelli A, Kissling WD, Flantua SGA, Bermúdez MA, Mulch A, Muellner-Riehl AN, Kreft H, Linder HP, Badgley C, Fjeldså J, Fritz SA, Rahbek C, Herman F, Hooghiemstra H and Hoorn C (2018) Geological and climatic influences on mountain biodiversity. *Nature Geoscience* **11**(10), 718–25. https://doi.org/10.1038/s41561-018-0236-z

Belmaker J and Jetz W (2011) Cross-scale variation in species richness-environment associations: Richness-environment scaling. *Global Ecology and Biogeography* **20**(3), 464–74. https://doi.org/10.1111/j.1466-8238.2010.00615.x

Benson RBJ, Butler R, Close RA, Saupe E and Rabosky DL (2021) Biodiversity across space and time in the fossil record. *Current Biology* **31**(19), R1225–R1236. https://doi.org/10.1016/j.cub.2021.07.071

Benton MJ (2009) The red queen and the court jester: species diversity and the role of biotic and abiotic factors through time. *Science* **323**(5915), 728–32. https://doi.org/10.1126/science.1157719

Bowman J (2003) Is dispersal distance of birds proportional to territory size? *Canadian Journal of Zoology* **81**(2), 195–202. https://doi.org/10.1139/z02-237

Bridle JR, Polechová J, Kawata M and Butlin RK (2010) Why is adaptation prevented at ecological margins? New insights from individual-based simulations. *Ecology Letters* **13**(4), 485–94. https://doi.org/10.1111/j.1461-0248.2010.01442.x

Cabral JS, Valente L and Hartig F (2017) Mechanistic simulation models in macroecology and biogeography: State-of-art and prospects. *Ecography* **40**(2), 267–80. https://doi.org/10.1111/ecog.02480

Catella SA and Abbott KC (2023) Effects of abiotic heterogeneity on species densities and interaction strengths lead to different spatial biodiversity patterns. *Frontiers in Ecology and Evolution* **11**, 1–16. https://doi.org/10.3389/fevo.2023.1071375

Ceresa F, Belda EJ and Monrós JS (2016) Similar dispersal patterns between two closely related birds with contrasting migration strategies. *Population Ecology* **58**(3), 421–27. https://doi.org/10.1007/s10144-016-0547-0

Chu JJ and Claramunt S (2023) Determinants of natal dispersal distances in North American birds. *Ecology and Evolution* **13**(2), e9789. https://doi.org/10.1002/ece3.9789

Claramunt S and Cracraft J (2015) A new time tree reveals Earth history's imprint on the evolution of modern birds. *Science Advances* **1**(11), e1501005. https://doi.org/10.1126/sciadv.1501005

Cohen JM and Jetz W (2024) Fine-Grain Predictions Are Key to Accurately Represent Continental-Scale Biodiversity Patterns. *Global Ecology and Biogeography* e13934. https://doi.org/10.1111/geb.13934

Connolly SR, Keith SA, Colwell RK and Rahbek C (2017) Process, Mechanism, and Modeling in Macroecology. *Trends in Ecology & Evolution* **32**(11), 835–44. https://doi.org/10.1016/j.tree.2017.08.011

Coyne JA, Orr HA, Coyne JA and Orr HA (2004) *Speciation*. Oxford University Press.

Dagallier L-PMJ, Janssens SB, Dauby G, Blach-Overgaard A, Mackinder BA, Droissart VSvenning J-C, Sosef MSM, Stévart T, Harris DJ, Sonké B, Wieringa JJ, Hardy OJ and Couvreur TLP (2020) Cradles and museums of

https://doi.org/10.1017/S0016756825100502 Published online by Cambridge University Press

generic plant diversity across tropical Africa. *New Phytologist* **225**(5), 2196–213. https://doi.org/10.1111/nph.16293

DeJong W and Degens H (2024) Micro- and Macroevolution: A Continuum or Two Distinct Types of Change? *Qeios*. https://doi.org/10.32388/KIEJWR.2

DeLong DC (1996) Defining Biodiversity. *Wildlife Society Bulletin (1973-2006)* **24**(4), 738–49.

deMenocal PB (2004) African climate change and faunal evolution during the Pliocene-Pleistocene. *Earth and Planetary Science Letters* **220**, 3–24. https://doi.org/10.1016/S0012-821X(04)00003-2

Dolson E. and Ofria C. (2021) Digital Evolution for Ecology Research: A Review. *Frontiers in Ecology and Evolution* **9**, 1–18. https://doi.org/10.3389/fevo.2021.750779

Doninck JV, Jones MM, Zuquim G, Ruokolainen K, Moulatlet GM, Sirén A, Cárdenas G, Lehtonen S and Tuomisto H (2020) Multispectral canopy reflectance improves spatial distribution models of Amazonian understory species. *Ecography* **43**(1), 128–37. https://doi.org/10.1111/ecog.04729

Fuchs J, Fjeldså J and Pasquet E (2006) An ancient African radiation of corvoid birds (Aves: Passeriformes) detected by mitochondrial and nuclear sequence data. *Zoologica Scripta* **35**(4), 375–85. https://doi.org/10.1111/j.1463-6409.2006.00238.x

Furness EN, Garwood RJ, Mannion PD and Sutton MD (2021a) Evolutionary simulations clarify and reconcile biodiversity-disturbance models. *Proceedings of the Royal Society B: Biological Sciences* **288**(1949), 20210240. https://doi.org/10.1098/rspb.2021.0240

Furness EN, Garwood RJ, Mannion PD and Sutton MD (2021b) Productivity, niche availability, species richness, and extinction risk: Untangling relationships using individual-based simulations. *Ecology and Evolution* **11**(13), 8923–40. https://doi.org/10.1002/ece3.7730

Furness EN and Sutton MD (2024) The biological cropping hypothesis over evolutionary time: An experimental test. *Theoretical Ecology* **17**(2), 121–29. https://doi.org/10.1007/s12080-024-00579-3

Garant D, Forde SE and Hendry AP (2007) The multifarious effects of dispersal and gene flow on contemporary adaptation. *Functional Ecology* **21**(3), 434–43. https://doi.org/10.1111/j.1365-2435.2006.01228.x

Garwood RJ, Spencer ART and Sutton MD (2019) REvoSim: Organism-level simulation of macro and microevolution. *Palaeontology* **62**(3), 339–55. https://doi.org/10.1111/pala.12420

Gotelli NJ, Anderson MJ, Arita HT, Chao A, Colwell RKConnolly SR, Currie DJ, Dunn RR, Graves GR, Green JL, Grytnes J-A, Jiang Y-H, Jetz W, Kathleen Lyons S, McCain CM, Magurran AE, Rahbek C, Rangel TFLV B, Soberón J, … **Willig MR** (2009) Patterns and causes of species richness: A general simulation model for macroecology. *Ecology Letters* **12**(9), 873–86. https://doi.org/10.1111/j.1461-0248.2009.01353.x

Graham CH and Hijmans RJ (2006) A comparison of methods for mapping species ranges and species richness. *Global Ecology and Biogeography* **15**(6), 578–87. https://doi.org/10.1111/j.1466-8238.2006.00257.x

Hillebrand H, Blasius B, Borer ET, Chase JM, Downing JA, Eriksson BK, Filstrup CT, Harpole WS, Hodapp D, Larsen S, Lewandowska AM, Seabloom EW, Van de Waal DB and Ryabov AB (2018) Biodiversity change is uncoupled from species richness trends: Consequences for conservation and monitoring. *Journal of Applied Ecology* **55**(1), 169–84. https://doi.org/10.1111/1365-2664.12959

Hughes C and Eastwood R (2006) Island radiation on a continental scale: Exceptional rates of plant diversification after uplift of the Andes. *Proceedings of the National Academy of Sciences* **103**(27), 10334–39. https://doi.org/10.1073/pnas.0601928103

Hurlbert AH and Jetz W (2007) Species richness, hotspots, and the scale dependence of range maps in ecology and conservation. *Proceedings of the National Academy of Sciences* **104**(33), 13384–89. https://doi.org/10.1073/pnas.0704469104

Jenkins CN, Pimm SL and Joppa LN (2013) Global patterns of terrestrial vertebrate diversity and conservation. *Proceedings of the National Academy of Sciences* **110**(28), E2602–E2610. https://doi.org/10.1073/pnas.1302251110

Jetz W, McPherson JM and Guralnick RP (2012) Integrating biodiversity distribution knowledge: Toward a global map of life. *Trends in Ecology & Evolution* **27**(3), 151–59. https://doi.org/10.1016/j.tree.2011.09.007

Jetz W, Rahbek C and Colwell RK (2004) The coincidence of rarity and richness and the potential signature of history in centres of endemism. *Ecology Letters* **7**(12), 1180–91. https://doi.org/10.1111/j.1461-0248.2004.00678.x

Karger DN, Conrad O, Böhner J, Kawohl T, Kreft H, Soria-Auza RW, Zimmermann NE, Linder HP and Kessler M (2017) Climatologies at high resolution for the earth's land surface areas. *Scientific Data* **4**(1), 170122. https://doi.org/10.1038/sdata.2017.122

Kevin Burke. (1996) The African Plate. *South African Journal of Geology* **99**(4), 341–409.

Koenig WD (1999) Spatial autocorrelation of ecological phenomena. *Trends in Ecology & Evolution* **14**(1), 22–26. https://doi.org/10.1016/S0169-5347(98)01533-X

Mannion PD, Upchurch P, Benson RBJ and Goswami A (2014) The latitudinal biodiversity gradient through deep time. *Trends in Ecology & Evolution* **29**(1), 42–50. https://doi.org/10.1016/j.tree.2013.09.012

Matthysen E (2012) Multicausality of dispersal: A review. In *Dispersal Ecology and Evolution* (eds J Clobert, M Baguette, TG Benton and JM Bullock). Oxford University Press. https://doi.org/10.1093/acprof:oso/9780199608898.003.0001

McCandlish DM (2011) Visualizing fitness landscapes. *Evolution* **65**(6), 1544–58. https://doi.org/10.1111/j.1558-5646.2011.01236.x

McGhee GR (2006) *The Geometry of Evolution: Adaptive Landscapes and Theoretical Morphospaces*. Cambridge University Press.

Mitchell MGE, Qiu J, Cardinale BJ, Chan KMA, Eigenbrod F, Felipe-Lucia MR, Jacob AL, Jones MS and Sonter LJ (2024) Key questions for understanding drivers of biodiversity-ecosystem service relationships across spatial scales. *Landscape Ecology***39**(2), 36. https://doi.org/10.1007/s10980-024-01842-y

Morales-Barbero J and Vega-Álvarez J (2019) Input matters matter: Bioclimatic consistency to map more reliable species distribution models. *Methods in Ecology and Evolution* **10**(2), 212–24. https://doi.org/10.1111/2041-210X.13124

Nathan R and Muller-Landau HC (2000) Spatial patterns of seed dispersal, their determinants and consequences for recruitment. *Trends in Ecology & Evolution* **15**(7), 278–85. https://doi.org/10.1016/S0169-5347(00)01874-7

Nathan R, Schurr FM, Spiegel O, Steinitz O, Trakhtenbrot A and Tsoar A (2008) Mechanisms of long-distance seed dispersal. *Trends in Ecology & Evolution* **23**(11), 638–47. https://doi.org/10.1016/j.tree.2008.08.003

Oliveros CH, Field DJ, Ksepka DT, Barker FK, Aleixo A, Andersen MJ, Alström P, Benz BW, Braun EL, Braun MJ, Bravo GA, Brumfield RT, Chesser RT, Claramunt S, Cracraft J, Cuervo AM, Derryberry EP, Glenn TC, Harvey MG., … **Faircloth BC** (2019) Earth history and the passerine superradiation. *Proceedings of the National Academy of Sciences* **116**(16), 7916–25. https://doi.org/10.1073/pnas.1813206116

O'Malley CPB, Roberts GG, Mannion PD, Hackel J and Wang Y (2023) Coherence of terrestrial vertebrate species richness with external drivers across scales and taxonomic groups. *Global Ecology and Biogeography* **32**(8), 1285–301. https://doi.org/10.1111/geb.13702

Pontarp M, Bunnefeld L, Cabral JS, Etienne RS, Fritz SA, Gillespie R, Graham CHHagen O, Hartig F, Huang S, Jansson R, Maliet O, Münkemüller T, Pellissier L, Rangel TF, Storch D, Wiegand T and Hurlbert AH (2019) The latitudinal diversity gradient: novel understanding through mechanistic eco-evolutionary models. *Trends in Ecology & Evolution* **34**(3), 211–23. https://doi.org/10.1016/j.tree.2018.11.009

Pontarp M and Wiens JJ (2017) The origin of species richness patterns along environmental gradients: Uniting explanations based on time, diversification rate and carrying capacity. *Journal of Biogeography* **44**(4), 722–35. https://doi.org/10.1111/jbi.12896

Porensky L. M. and Young T. P. (2013) Edge-Effect Interactions in Fragmented and Patchy Landscapes. *Conservation Biology* **27**(3), 509–19. https://doi.org/10.1111/cobi.12042

Rangel TF, Edwards NR, Holden PB, Diniz-Filho JAF, Gosling WD, Coelho MTP, Cassemiro FAS, Rahbek C and Colwell RK (2018) Modeling the ecology and evolution of biodiversity: Biogeographical cradles, museums, and graves. *Science* **361**(6399), eaar5452. https://doi.org/10.1126/science.aar5452

Ruffley M, Peterson K, Week B, Tank DC and Harmon LJ (2019) Identifying models of trait-mediated community assembly using random forests and

https://doi.org/10.1017/S0016756825100502 Published online by Cambridge University Press

approximate Bayesian computation. *Ecology and Evolution* **9**(23), 13218–30. https://doi.org/10.1002/ece3.5773

Stein A, Gerstner K and Kreft H (2014) Environmental heterogeneity as a universal driver of species richness across taxa, biomes and spatial scales. *Ecology Letters* **17**(7), 866–80. https://doi.org/10.1111/ele.12277

Stein A and Kreft H (2015) Terminology and quantification of environmental heterogeneity in species-richness research. *Biological Reviews* **90**(3), 815–36. https://doi.org/10.1111/brv.12135

Sutherland GD, Harestad AS, Price K and Lertzman KP (2000) Scaling of Natal Dispersal Distances in Terrestrial Birds and Mammals. *Conservation Ecology* **4**(1), 16. https://doi.org/10.5751/ES-00184-040116. http://www.consecol.org/vol4/iss1/art16/

Tuanmu M-N and Jetz W (2015) A global, remote sensing-based characterization of terrestrial habitat heterogeneity for biodiversity and ecosystem modelling. *Global Ecology and Biogeography* **24**(11), 1329–39. https://doi.org/10.1111/geb.12365

van der Plas F, Janzen T, Ordonez A, Fokkema W, Reinders J, Etienne RS and Olff H (2015) A new modeling approach estimates the relative importance of different community assembly processes. *Ecology* **96**(6), 1502–15. https://doi.org/10.1890/14-0454.1

Willig MR, Kaufman DM and Stevens RD (2003) Latitudinal gradients of biodiversity: pattern, process, scale, and synthesis. *Annual Review of Ecology, Evolution, and Systematics* **34**, 273–309. https://doi.org/10.1146/annurev.ecolsys.34.012103.144032

Zera AJ and Brisson JA (2012) Quantitative, physiological, and molecular genetics of dispersal/migration. In *Dispersal Ecology and Evolution* (eds J Clobert, M Baguette, G Benton and JM Bullock). Oxford University Press. https://doi.org/10.1093/acprof:oso/9780199608898.003.0006

https://doi.org/10.1017/S0016756825100502 Published online by Cambridge University Press